Journal of Materials Chemistry A

ROYAL SOCIETY OF CHEMISTRY

PAPER

View Article Online
View Journal | View Issue

Cite this: J. Mater. Chem. A, 2026, 14, 8846

Next generation solid amine sorbents for scalable direct air capture of carbon dioxide

Zhijian Wan, *[a] Cameron White,[a] Jason Czapla,[a] Bobby Pejcic,[b] Wendy Tian,[c] Durga Acharya,[c] Sophia Surin,[d] Wei Wu[e] and Colin D. Wood *[a]

Received 11th December 2025
Accepted 23rd January 2026

DOI: 10.1039/d5ta10113a

rsc.li/materials-a

Direct air capture (DAC) is crucial for mitigating climate change by directly removing CO_2 from the atmosphere. However, the large-scale deployment of DAC is hindered by the lack of durable and scalable sorbents and processes especially materials that comply with green synthesis principles. Here, we have applied these principles to develop a simple, scalable method for synthesising a novel sorbent, a nitrogen-rich solid amine network (SAN) with unique structure having an internal mesh size around 0.5 nm. The synthesis is green and can be completed within 10 minutes under ambient conditions. The sorbent showed a CO_2 uptake capacity up to 3.11 mmol g^{-1} under real-world DAC conditions, nearly three times higher than that of conventional SiO_2-impregnated sorbents. It also demonstrated remarkable resistance to oxidative degradation, retaining over 75% of its capacity after 7 days of accelerated ageing under elevated temperatures (85 °C) in air, while conventional impregnated sorbents and commercially available resins incurred a greater than 50% reduction. In a proof-of-concept DAC scenario assisted by solar, the sorbent was directly exposed to outdoor air and achieved 1 mmol g^{-1} CO_2 uptake in just 5 hours. This novel sorbent shows promise for large-scale DAC systems by tackling key DAC-associated challenges.

Introduction

Direct air capture (DAC) is a process where CO_2 is captured directly from the atmosphere, serving as a carbon dioxide removal (CDR) technology to address legacy CO_2 to achieve negative emissions.[1,2] DAC offers several advantages, including (i) less land requirements compared to natural CDR methods like afforestation and reforestation; (ii) no geographical limitations, allowing DAC facilities to be built in locations where renewable energy sources or storage/utilisation options are available; and (iii) the ability to offset hard-to-abate emissions. Despite its potential, the deployment of large-scale DAC remains slow, primarily due to the lack of reliable sorbents with high capture capacity and stability, which leads to high energy consumption and costs. For instance, using aqueous hydroxide for DAC requires a regeneration temperature up to 900 °C, and the overall cost with current technologies exceeds $400 per t CO_2,[3] four times higher than the targeted $100 per t CO_2 to make DAC economically viable.[4]

Considerable efforts to explore new sorbents are crucial for accelerating the development of DAC. Although the aqueous hydroxide slurry has been commercially adopted, its high regeneration temperature (up to 900 °C) and the need to burn natural gas for heat present significant obstacles to the process.[5] Amines, however, present an alternative option owing to their high affinity for CO_2 and lower regeneration temperatures (typically around 110 °C). In fact, aqueous amine solutions have been widely used in the industry for post combustion capture.[6] However, this aqueous system is not directly applicable to DAC due to the ultra-low CO_2 concentration (approximately 0.04%) in the air, which results in slow absorption kinetics.[7] In addition, aqueous amine sorbents also suffer from evaporation of water and amines, amine-induced facility corrosion, and degradation in oxidative environments.[8] To overcome these challenges for DAC, amines are typically incorporated into porous solids, which minimises volatility, enhances stability, and improves the accessibility of amine sites to CO_2.[8–12]

The incorporation of amines into solid supports can be achieved through three approaches, including (I) direct impregnation through physically mixing amines with mesoporous silica (MCM-41, SBA-15),[13,14] zeolites,[15,16] resins,[17] and metal organic frameworks (MOF);[18,19] (II) covalent tethering through chemical bonding between aminosilanes and silanol

[a]Energy Business Unit, Commonwealth Scientific Industrial Research Organisation (CSIRO), Kensington, Western Australia 6151, Australia. E-mail: zhijian.wan@csiro.au; colin.wood@csiro.au

[b]Mineral Resources, Commonwealth Scientific Industrial Research Organisation (CSIRO), Kensington, Western Australia 6151, Australia

[c]Manufacturing, Commonwealth Scientific Industrial Research Organisation (CSIRO), Clayton, Victoria 3168, Australia

[d]Mineral Resources, Commonwealth Scientific Industrial Research Organisation (CSIRO), Waterford, Western Australia 6152, Australia

[e]Shenzhen Institutes of Advanced Technology, Chinese Academy of Sciences, Shenzhen, 518055, P. R. China

groups on the surface of silica support;[20,21] and (III) *in situ* polymerisation through ring opening of aziridine to produce nitrogen-rich hyperbranched aminosilica.[20,22] These three classes of solid sorbents have their own advantages and limitations. Class I sorbents offer the advantage of simple preparation and exhibit high CO_2 capture capacities exceeding 2 mmol g^{-1} (under 400 ppm CO_2).[23,24] However, they often suffer from amine leaching due to weak interactions between the amines and the porous supports, as well as issues with pore blockage.[25] Class II and III sorbents eliminate the leaching of amines thanks to the chemical immobilisation of amines onto the supports. However, these two types of materials often exhibit low CO_2 uptake, typically below 1 mmol g^{-1} under DAC conditions.[26,27] Furthermore, all three classes of sorbents rely on porous materials as the supports, which are prone to trap water in their pores to form plugs. Additionally, the synthesis of many porous supports often involves either complex procedures or harsh reaction conditions, rendering them less practical for the implementation of DAC.

Recently, sorbents without the usage of an extra support have emerged as promising candidates for post combustion capture.[28–30] The sorbents are prepared through an ice-templating approach, in which branched polyethyleneimine (PEI) is crosslinked in aqueous solution under freezing conditions (<−10 °C), while the formation of ice crystals acted as a scaffold or porogen. The reaction leads to the creation of a PEI-based porous monolith upon thawing the sample at room temperature. This monolith could achieve a remarkable CO_2 uptake of 5.5 mmol g^{-1} under 10% CO_2 with 65% relative humidity.[29] Despite this promising performance, the absence of data for the monolith used in DAC may imply that such sorbent is inefficient for capturing ultra-diluted CO_2. Moreover, large-scale deployment of DAC requires sorbents that can be mass-produced using low-cost processes, such as simple synthesis routes without post-synthesis solvent washing.

We have previously reported a support-free DAC sorbent prepared *via* a one-pot crosslinking reaction that can be completed within 24 hours under ambient conditions.[31] In this present work, we develop a new class of sorbents that can be synthesised in as little as 10 minutes, substantially enhancing their potential for large-scale DAC deployment. This sorbent is a solid amine network (SAN) that combines the advantages of Class I–III sorbents, namely the high CO_2 capture capacity of Class I and the enhanced stability associated with Class II and III, and accordingly, it is designated as Class IV sorbent. The SAN is self-supported without the need for a porous support and can be easily obtained through a one-pot synthesis process under ambient conditions. This synthesis method involves no complex or solvent-intensive purification so is environmentally favourably. As such the method aligns with the majority of the twelve green chemistry principles.[32] The new sorbent demonstrated exceptional CO_2 capture capacity under real-world DAC conditions, and equally importantly, the sorbent also exhibited remarkable stability under oxidative conditions compared to those prepared *via* conventional methods.

Experimental

Materials

All chemicals were purchased from Sigma-Aldrich and used without further treatment, including triglycidyl isocyanurate (TGIC), branched polyethyleneimine (PEI25000, M.W. ~25 000), branched polyethyleneimine (PEI800, M.W. ~800), methyldiethanolamine (MDEA, 99%), diethanolamine (DEA, reagent grade, ≥98.0%), triethanolamine (TEA, reagent grade, ≥98.0%), silica (SiO_2, high purity grade), Lewatit VP OC 1065 ion exchange resin (Lewatit, spherical beads, 0.5 mm in diameter), trisodium phosphate (TSP, 96%).

Synthesis of Class IV solid amine network (SAN) sorbents

The synthesis of Class IV sorbents was performed in a 100 mL Schott bottle. In the case of using TEA as the swelling agent, 10 g of PEI25000, 2 g of TGIC, 0.05 g of TSP (as an iron chelator) and 12 g of TEA were added to the bottle. The mixture was vigorously stirred at 800 rpm under ambient conditions using a mechanical PTFE stirring shaft. This process resulted in the formation of a gel, which was then solidified and broken down into a powder with particle sizes ranging from 200 to 500 μm. The resulted sorbent was denoted as TEA@SAN.

Following the same strategy, sorbents based on MDEA, DEA, mixtures of 50%DEA & 50% TEA, and 50%DEA & 50% MDEA were also prepared. These samples were denoted as MDEA@SAN, DEA@SAN, 0.5DEA&0.5TEA@SAN, 0.5DEA&0.5MDEA@SAN, respectively.

In addition, dry SAN was prepared using ethanol instead of an ethanolamine, which was removed in an oven at 70 °C upon completion of the reaction. H_2O@SAN was subsequently prepared by mixing distilled water with the dry SAN at a 1 : 1 weight ratio.

Preparation of silica (SiO_2) supported sorbents

For comparison, Class I sorbents were prepared by impregnating mesoporous silica with various liquids at a weight ratio of 1 : 1. The liquids include DEA, MDEA, TEA, and PEI800. The samples were denoted as DEA/SiO_2, MDEA/SiO_2, TEA/SiO_2, and PEI800/SiO_2, respectively.

Material characterisation

The viscosity evolution of the synthesis formulation was measured using a Fann viscometer (Model 286), with the bob initially rotating at 15 rpm. It should be noted that this lower rotation speed led to a longer apparent reaction time compared with the actual synthesis procedure, in which the mixture was stirred at 800 rpm.

Fourier-transform infrared (FTIR) spectroscopy analysis was used to monitor the synthesis reaction with particular focus on the consumption of TGIC, as well as the sorbent degradation under oxidative conditions. The FTIR spectrometer (Thermo Scientific Nicolet Summit) was equipped with attenuated total reflectance (ATR) correction and recorded the spectrum in the range of wavenumber 400 to 4000 cm^{-1}.

Thermogravimetric analysis-mass spectrometry (TGA-MS, Netzsch STA 449 F3 Jupiter with QMS 403 Quadro Aeolos) was employed to measure the temperature of CO_2 and water desorbed from 0.5DEA&0.5TEA@SAN. Approximately 20 mg of CO_2 saturated 0.5DEA&0.5TEA@SAN was loaded in an alumina crucible for the measurement. The TGA was heated in the temperature range of 35 to 110 °C (heating rate of 1 °C min^{-1}) under nitrogen at a flow rate of 40 mL min^{-1}. The mass signal of the desorbed CO_2 was recorded using a quadrupole mass spectrometer and the temperature at which the mass signal detected was considered as the CO_2 desorption temperature.

The BET specific area and the pore size distribution of the samples were determined by N_2 physisorption using Micromeritics ASAP2020 at −196 °C maintained by liquid nitrogen. The samples were activated in seal-frit capped tubes on the degassing port of the ASAP 2020. In the case of the SAN, the sample was degassed at 90 °C under vacuum for 5 hours, while SiO_2 was degassed at 200 °C under vacuum for 10 hours. After activation, the sample tubes were backfilled with helium to atmospheric pressure before the sorption measurements. An equilibration interval of 30 s and a relative pressure tolerance of 5% were employed in these tests.

Thermoporometry was performed to examine changes in the freezing point of the swollen liquid when confined using differential scanning calorimetry (DSC) analyses (Mettler Toledo DSC30 with "Star Software" version 16.3). The system was calibrated using the total *n*-octane/indium method. An empty aluminium pan served as the reference, while approximately 20 mg of sample containing 50% of water was encapsulated in another pan for the measurements. The DSC scans were conducted over a temperature range of −60 °C to 25 °C, at a heating rate of 10 °C min^{-1}, with nitrogen used as the environmental gas.

The average pore size and distribution were analysed using Positron Annihilation Lifetime Spectroscopy (PALS). Measurements were performed with EG&G Ortec spectrometers set in fast–fast coincidence mode. Sample of 2 mm thickness was placed on each side of a ^{22}NaCl positron point source, encapsulated in a Mylar envelope. Data acquisition involved a minimum of ten measurements at room temperature, each comprising 1×10^6 integrated counts.

Spectral analysis was conducted using LTv9 software, where the data were fitted to three lifetime components. The first component, fixed at 125 ps, corresponded to the annihilation of para-positronium (pPs), a bound state of a positron and an electron with opposite spin. The second component, approximately 400 ps, was associated with the direct annihilation of positrons with free electrons in the sample. The third and longest lifetime component (τ_3) represented the annihilation of ortho-positronium (oPs), a bound state of a positron and an electron with the same spin, and the relative intensity I_3 of oPs lifetime is related to the average number of pores in the sample. The oPs lifetime (τ_3) was used to calculate the average free volume diameter (d) *via* the Tao–Eldrup equation and the PAScual software was adapted to calculate pore size distributions.

Evaluation of sorbent performance in real-world DAC

The CO_2 capture performance of the adsorbents in DAC was evaluated using an in-house built test instrument. A blank run without sorbent loading was initially performed to validate the method, giving a CO_2 uptake of 0.05 mmol g^{-1}, and therefore, the CO_2 capture capacity of the sorbents was levelized to have 0.05 mmol g^{-1} deducted. For each measurement, the sorbent was regenerated in a fan-forced oven at 85 °C in air under ambient pressure for 1 h to remove pre-adsorbed CO_2 and moisture, and then 5 g of the dried sample was loaded into the test instrument. Humidified air contained 500 mL min^{-1} of compressed ambient air and 500 mL min^{-1} of water saturated air was introduced into the tube, making up a total air flow rate of 1000 mL min^{-1} (a gas hourly space velocity, GHSV of 12 000 mL min^{-1} g^{-1}) at ambient conditions. The details of the setup and the methodology of calculating CO_2 and H_2O uptake can be found in our earlier publication.[31]

Furthermore, we also evaluated the sorbent performance under real-world DAC conditions. Specifically, 15 g of dried 0.5DEA&0.5TEA@SAN was spread in a tray (100 × 100 × 5 mm), which was positioned in front of a computer fan. This setup was placed outdoor in an open area. A monocrystalline solar panel was used to power the fan at a wind speed in the range of 1.5 to 2 m s^{-1}. Samples were collected from five different spots on the tray, including the four corners and the centre, at one-hour intervals for 5 hours. These samples were then mixed and analysed using a thermalgravimetric analysis (TGA, Netzsch, STA 449 F3) coupled with a CO_2 sensor (Vaisala GMP252) at its exit. The TGA was heated up to 90 °C (heating rate of 5 °C min^{-1}) under nitrogen (99.99%) at a flow rate of 60 mL min^{-1}. The concentration of the desorbed CO_2 (ppm) was recorded by the sensor as a function of time and the amount of CO_2 was then calculated.

CO_2 adsorption kinetics

The equilibrium adsorption behaviour and time-dependent kinetics are determined by the gas–solid interfacial adsorption kinetics model combining pseudo-first-order kinetic model[33] and Langmuir isotherm equation[34] as:

$$q_t = q_e \frac{Kc}{1 + Kc}\left(1 - e^{-k_1 t}\right)$$

where t is the adsorption time, q_t is the adsorbed amount of CO_2 at time t (h). q_e is the equilibrium adsorption capacity (mmol g^{-1}). c is the inlet CO_2 concentration (ppm). K is the adsorption equilibrium constant of Langmuir type (ppm^{-1}), and k_1 is the kinetic rate constant for adsorption (h^{-1}).

Evaluation of sorbent stability through accelerated ageing

The stability of the Class IV adsorbents was assessed through accelerated ageing and compared with the SiO_2 supported adsorbents. All samples were placed in a fan-forced oven at 85 °C in air for seven days. The CO_2 capture capacity of the aged samples was evaluated using the same approach as previously described. The 0.5DEA&0.5TEA@SAN and 0.5DEA&0.5MDEA@SAN samples were tested daily, while the other samples

were assessed only at the end of the ageing process. In addition, the mass loss of the SAN sorbents before and after the ageing are also recorded.

Results and discussion

Synthesis of solid amine network (SAN)

The synthesis of the SAN was carried out through a step-growth ring-opening polymerisation process, using triglycidyl isocyanurate (TGIC) as the crosslinker and polyethyleneimine (PEI25000) as the monomer. Fig. 1a shows the structures of TGIC, PEI25000 and the synthesis route of the SAN. TGIC possesses three oxirane rings, which are very reactive owing to the high strain energy of the three-membered ring.[35] PEI25000 is a branched polyamine containing primary, secondary and tertiary amine groups with approximate proportion of 1 : 2 : 1. The polymerisation reaction proceeds *via* nucleophilic attack of the amine groups in PEI25000 on the electrophilic carbon of the oxirane rings, resulting in ring opening with the cleavage of C–O bond, and concurrently, the formation of a C–N bond. The reaction proceeds through three stages (pregelation, active network growth and vitrification), resulting in formation of crosslinks and chain growth, which are reflected in the changes in viscosity of the synthesis mixture measured using a viscometer shown in Fig. 1b. During the pregelation stage, an induction period is observed with no significant changes in viscosity. This is followed by a sharp viscosity increase, indicating a rise in molecular weight and the formation of large molecules (active network growth stage). The reaction then advances to the vitrification stage to form a glassy solid (evidenced by immobility of viscometer measuring bob), and eventually, yields a self-supported nitrogen-rich solid amine network with PEI25000 being knitted together by TGIC, as illustrated in Fig. S1.

Due to the high nucleophilicity of the amine groups and the strong electrophilicity of the epoxy groups, the reaction was conducted *via* a one-step process in which all reagents are mixed and the reaction occurs under ambient conditions without requiring any catalysts or initiators. In fact, the ring-opening reaction simultaneously generates hydroxyl groups, which can form hydrogen bonds with the oxygen atoms of unreacted epoxy groups, further promoting nucleophilic attacks by the amines on the oxirane rings. Consequently, the reaction was autocatalytic and can be completed in as little as 10 minutes. Movie S1 demonstrates this "all-in" process for the synthesis of TEA@SAN using triethanolamine (TEA) as the agent. The reaction mixture reached a gel point after approximately 7 minutes, subsequently followed by a transition to a glassy state. This solid was immediately broken into a powder due to the shearing force from the stirring shaft. At the conclusion of the reaction, no waste was produced. The sorbent can be used directly for DAC without the need for further treatment, such as separation or purification.

This reaction kinetics were monitored by changes in infrared (IR) absorption related to the oxirane ring and hydroxy groups over the course of the reaction (Fig. 1c–e). The peak at 843 cm^{-1}, attributed to the C–O–C stretching of the oxirane ring, gradually

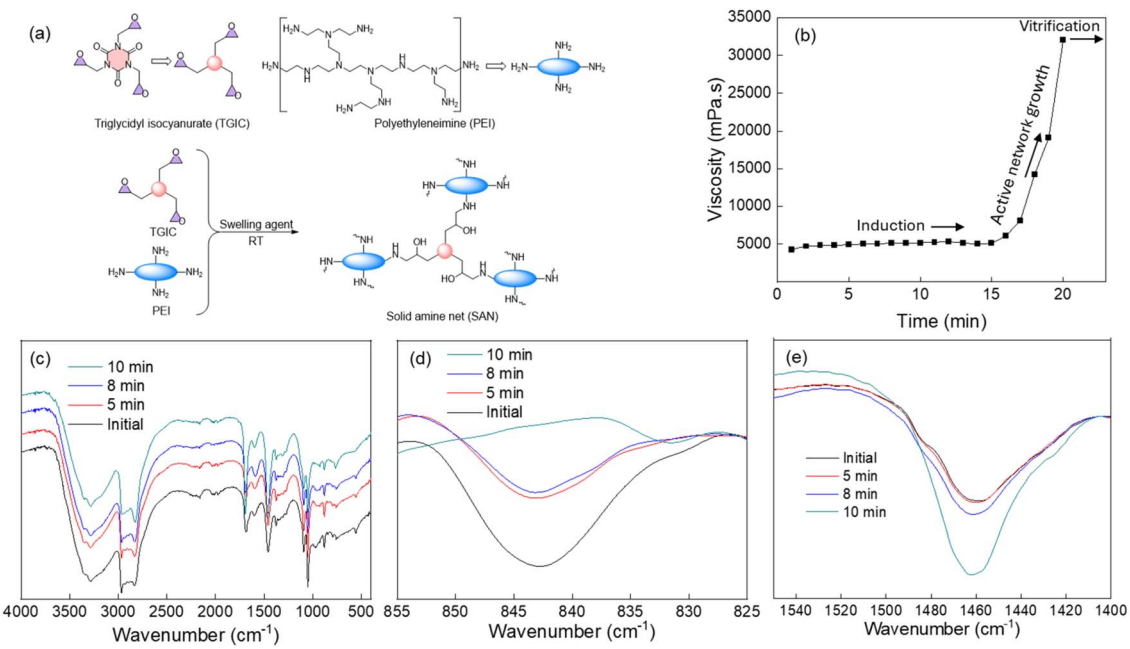

Fig. 1 Schematic of the synthesis, change in viscosity and evolution of infrared (IR) absorption of functional groups during the synthesis of the SAN: (a) TGIC as a crosslinker to react with PEI25000, forming a nitrogen-rich solid amine network at ambient conditions; (b) viscosity of the synthesis mixture; (c) full IR spectra in the range of wavenumber 400–4000 cm^{-1}; (d) IR spectra for C–O–C stretching of the oxirane ring (843 cm^{-1}), which is gradually decreased in intensity and disappeared at the 10 minute mark, indicating the consumption of epoxy groups (ring opening) and completion of the reaction; (e) IR spectra for the C–N stretch vibration (1460 cm^{-1}) with an increase in intensity attributing to the formation of C–N bonds between TGIC and PEI.

decreased in intensity and disappeared at the 10 minute mark (Fig. 1d), indicating the consumption of epoxy groups (ring opening) and completion of the reaction, both showing fast kinetics. Correspondingly, an increase in the intensity of a peak at 1460 cm^{-1} was also observed, which is most likely attributed to a C–N stretch vibration arising from the reaction between amine groups in PEI with the epoxide (Fig. 1e).[36]

All Class IV sorbents specified in this study can be prepared through this one-pot process, using the desired agents such as methyldiethanolamine (MDEA), diethanolamine (DEA), and even water. It should be noted that in the case of using DEA, the gelation time was approximately 2 minutes longer than that compared to those containing tertiary amines such as TEA and MDEA. This can be attributed to the presence of a secondary amine group in DEA, which may react directly with the epoxide groups of TGIC, thereby consuming part of the crosslinker and leading to a slightly slower polymerisation process. In contrast, tertiary amines typically act as catalysts that facilitate the ring-opening of epoxide groups, thereby accelerating the polymerisation reaction.[37,38]

The outlined synthesis method satisfies a number of the twelve principles of green chemistry,[32] as summarised in Table S1. Owing to the simplicity of the synthesis method, Class IV sorbent could be mass-produced economically and in an environmentally friendly manner. Using similar synthesis strategies, our group produced 2 tonnes of a proprietary sorbent in one month (20 kg per batch, with 5 batches per day) to support a pilot-scale DAC unit. To the best of the authors' knowledge, this is the first time reporting production of such large quantity of DAC sorbent at a lab-scale. It can be foreseen that an industrial-scale synthesis plant could manufacture tonnes of material daily.

Characterisation of Class IV sorbents

The epoxide-amine curing reaction is known to form a 3D network architecture.[39,40] However, direct characterisation of the network is challenging primarily due to the insolubility and infusibility of the polymer. Herein, we employed thermoporometry and positron annihilation lifetime spectroscopy (PALS) to further characterise the SANs.

Thermoporometry is an efficient method to characterise the pore structure of a solid by measuring the changes in freezing point of a liquid confined within pores.[41] In this study, water was used as the probe liquid to incorporate into the SAN network for the measurement, and compared with that of water in SiO_2. The DSC curves for H_2O@SAN and H_2O/SiO_2 are shown in Fig. 2a. A large exothermic peak with an onset temperature of −22.5 °C was observed for H_2O/SiO_2. The peak is associated with ice formation, and the depression of the water freezing point to −22.5 °C corresponds to a pore size of roughly 5 nm for SiO_2 according to a previously reported study.[42] This closely matches with the pore size of SiO_2 (6.04 nm) measured from nitrogen physisorption shown in Fig. 2b (adsorption/desorption isotherms) and Fig. 2c (pore size distributions). On the other

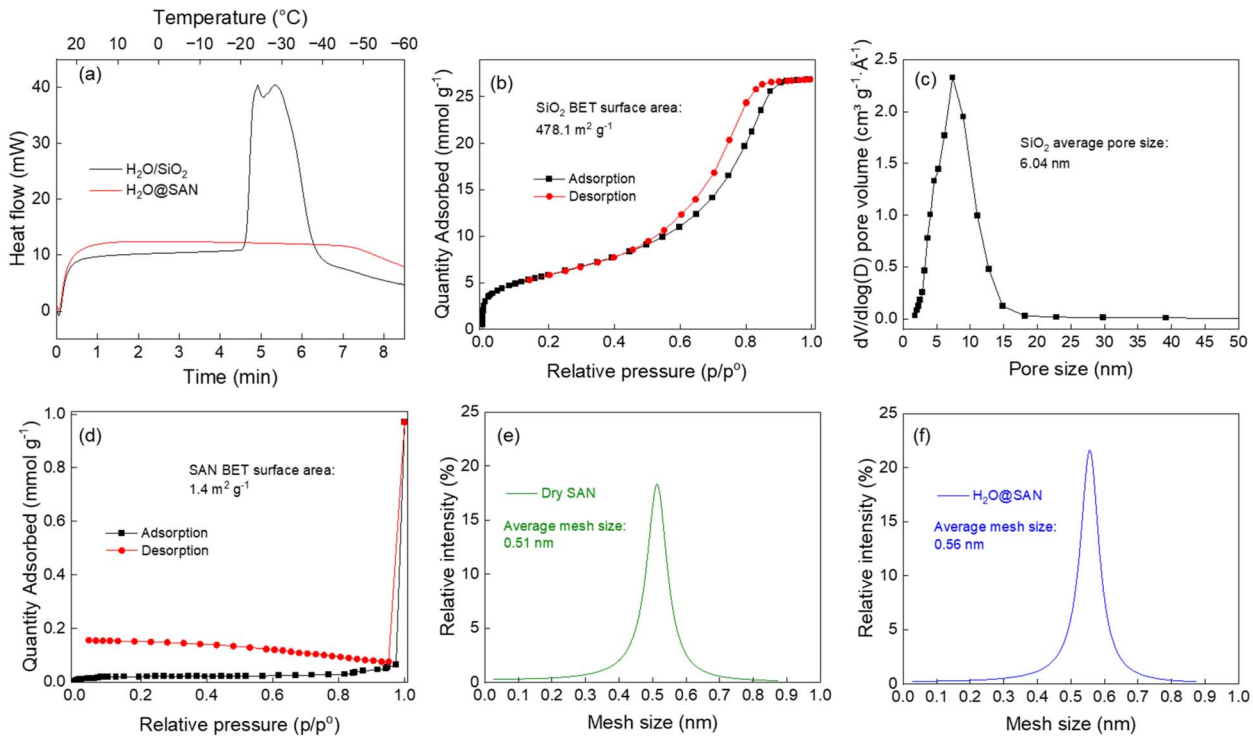

Fig. 2 Structural properties of SAN measured by thermoporometry and nitrogen physisorption and compared to SiO_2. (a) DSC curves to measure the depression in freezing point of water when confined in SiO_2 and SAN; (b) adsorption/desorption isotherms for SiO_2, (c) pore size distribution of SiO_2; (d) adsorption/desorption isotherms for SAN; (e) mesh size distribution for dry SAN; and (f) mesh size distribution for H_2O@SAN measured using PALS.

hand, no such exothermic peak was found in the DSC curve for H_2O@SAN, indicating that the water incorporated into the SAN matrix cannot freeze even at temperatures as low as −60 °C. This suggests that water underwent substantial changes to its properties when confined in the SAN. The interaction between the water molecules and the SAN is stronger than the intramolecular interaction between water molecules and combined with the individually immobilised species the formation of ice is inhibited. However, SAN is virtually non-porous according to Fig. 2d, it thus raises a question why it can exert stronger confinement effects than that of SiO_2 with well-defined pores.

We then employed PALS to measure the mesh size of the SAN matrix. As shown in Fig. 2e dry SAN has an average mesh size of 0.51 nm, and 0.56 nm for H_2O@SAN (Fig. 2f). A slight increase in mesh size of H_2O@SAN is a result of chain expansion by incorporating water that leads to an increase in free voids within the matrix. Nevertheless, the PALS results reveal that SAN possess sub-nanometre networks. When confined within such a small scale network, water molecules are strongly bounded to the network through hydrogen bonding, likely individually immobilised and thus non-freezable,[43,44] which is consistent with the DSC thermoporometry with no detectable exothermic peak.

The unique structure of the SAN distinguishes it as a novel class of sorbent materials different from conventional counterparts relying on porous support. The confinement effect of SAN on the swollen liquids as well as its impact on CO_2 uptake and stability are discussed in the following section.

CO_2 capture capacity of Class IV sorbents in DAC

In this study, the CO_2 capture capacity of the SAN sorbents in DAC was assessed under ambient conditions with humidified ambient air used as the feedstock, reflecting actual DAC with ultra-diluted CO_2 and ample humidity.

Fig. 3 illustrates the CO_2 uptake of Class IV sorbents in DAC, compared to SiO_2 impregnated counterparts (Class I) as well as a commercially available Lewatit resin. When using TEA and MDEA as the swelling agent, the resulted sorbents, TEA@SAN and MDEA@SAN, show CO_2 uptakes of 1.20 and 1.50 mmol g^{-1}, respectively. Considering that these two agents are virtually inert in capturing CO_2 from air as evidenced by their conventional Class I counterparts TEA/SiO_2 (0.06 mmol g^{-1}) and MDEA/SiO_2 (0.09 mmol g^{-1}), the high capture capacity of TEA@SAN and MDEA@SAN is primarily attributed to the amine groups inherited from PEI. In addition, the hydroxyl groups in TEA and MDEA can also contribute to CO_2 capture by facilitating noncovalent interactions with CO_2 *via* hydrogen bonding, akin to the role polyethylene glycol (PEG) plays in enhancing the CO_2 capture capacity of PEI.[45]

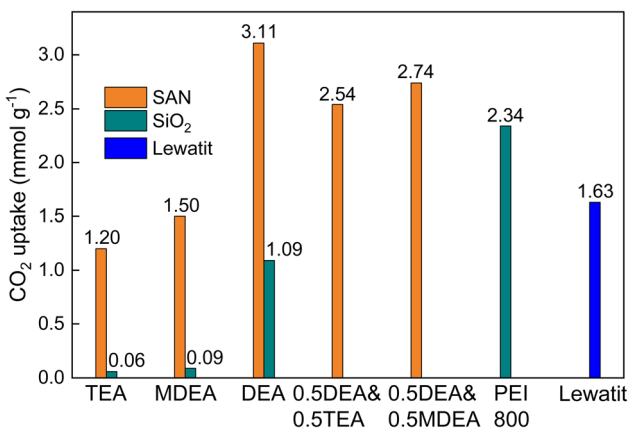

Fig. 3 CO_2 capture capacity of the Class IV sorbents with different swelling agents. The sorbents show remarkable CO_2 uptake in DAC up to 3.11 mmol g^{-1} under practical conditions, outperforming Class I counterparts and the commercially available Lewatit resin.

The capture capacity of the Class IV sorbents can be further increased by incorporating an active amine (DEA) as the swelling agent. DEA@SAN exhibits an exceptionally high CO_2 uptake of 3.11 mmol g^{-1}, which is 2.9 times higher than its Class I counterparts, DEA/SiO_2 (1.09 mmol g^{-1}). Additionally, it also outperforms other sorbents, being 1.3 times higher than the widely studied PEI-based sorbent (2.34 mmol g^{-1} for PEI800/SiO_2), 1.9 times higher than the Lewatit resin (1.63 mmol g^{-1}), and 1.5 times higher than the recently reported COF-999 (2.05 mmol g^{-1}).[46] The two sorbents, 0.5DEA&0.5TEA@SAN and 0.5DEA&0.5MDEA@SAN, also demonstrate higher CO_2 uptake of 2.54 and 2.74 mmol g^{-1}, respectively. Furthermore, the SAN sorbents exhibit rapid capture kinetic, as demonstrated in Movie S2, which shows the dynamic changes in CO_2 and water concentrations at the inlet and outlet for DEA@SAN. The outlet CO_2 concentration drops sharply to 0 ppm when the air stream had been contacted with the sorbent, indicating efficient and immediate CO_2 removal. Additional details, including inlet and outlet CO_2 and water concentrations before and after passing through the sorbents during the DAC test, as well as the CO_2 and water uptake as a function of time for each sorbent can be found in Fig. S2–S11. New species attributed to CO_2 adsorption during DAC for DEA@SAN are identified by IR and shown in Fig. S12, in which the peak at 1549 cm^{-1} corresponds to COO– asymmetric stretch and that at 1410 cm^{-1} is for COO– symmetric stretch along with CO_3^{2-}/HCO_3^- skeletal, indicating the formation of carbamate and carbonate/bicarbonate species.[1,36]

These results demonstrate that Class IV sorbents are highly effective for DAC. DEA@SAN with 3.11 mmol g^{-1} capture capacity ranks among the highest reported to date. Theoretically, two DEA molecules can react with one CO_2 molecule through primarily forming ammonium carbamate,[47] giving DEA a maximum capture capacity of 4.76 mmol g_{DEA}^{-1}. On the other hand, H_2O@SAN shows CO_2 uptake of 0.75 mmol g^{-1} (Fig. S13), making that the contribution from DEA in DEA@SAN is 2.36 mmol g^{-1}, equivalent to 4.72 mol g_{DEA}^{-1} when normalised to DEA content, as water does not participate in capturing CO_2. This corresponds to nearly 100% amine efficiency of DEA when incorporated into SAN. By contrast, DEA impregnated into SiO_2 (DEA/SiO_2) achieves only 1.09 mmol g^{-1} (2.18 mmol g_{DEA}^{-1}), corresponding to a capture efficiency of 45.7%.

Moreover, the kinetic parameters for all sorbents summarised in Table S2, together with the fitted adsorption results in Fig. S2–S11 further confirm the high CO_2 uptake capacity for the

Class IV sorbents. With higher q_e and K values of Class IV than Class I counterparts (except PEI800/SiO_2), this suggests that Class IV sorbents are particularly effective for capturing ultra-diluted CO_2. Although PEI800/SiO_2 and Lewatit resin also display comparatively higher q_e and K, their insufficient stability (as discussed in the next section) renders them unsuitable for practical DAC deployment.

This high capture capacity can be credited to the unique structure of the SAN network as aforementioned. The cross-linking of TGIC with PEI leads to chain growth, with chemical chains connected to form network loops in sub-nanometre size (Fig. 2e). Meanwhile, the amines (TEA, MDEA, DEA) are incorporated into these networks through strong hydrogen bonding with the network functional groups (–OH and –NH–). As displayed in Fig. 4a, pure DEA exhibited two distinct peaks at 3306 and 3357 cm^{-1}, corresponding to the N–H and O–H stretching vibrations, respectively. Upon incorporation into the SAN (DEA@SAN), the O–H stretching peak diminished, while a new band appeared at 3177 cm^{-1}, which is absent in the dry SAN. This shift is attributed to hydrogen bond formation between DEA and SAN, resulting in a red shift of the O–H stretch to lower wavenumbers. When hydrogen bonded and confined within such a small space, the intramolecular interactions between DEA molecules are disrupted. Instead, single DEA molecules would be individually immobilised and undergo dramatic changes (similar as water in H_2O@SAN). This permits the exposure of all DEA molecules to CO_2, achieving virtually 100% utilisation efficiency, as illustrated in Fig. 4b. In comparison, DEA impregnated into SiO_2 still retains its original characteristics as evidenced by the two N–H and O–H stretching vibrations in DEA/SiO_2 (Fig. 4c), indicating weak interactions between DEA molecules and the pore walls of SiO_2, which would inevitably form DEA aggregates that plug the pores,[48,49] resulting in DEA being inaccessible for CO_2 and therefore low utilisation efficiency, as demonstrated in Fig. 4d.

It is also worth noting that the Class IV sorbents are tolerant to water. The sorbents showed water uptake around 30 wt% after the DAC test as illustrated in Fig. S2–S11d. However, the SAN remained virtually the same as its initial state without visible changes in morphology. Such high water tolerance of the SAN sorbents is not possible for other classes of DAC sorbent which are rendered ineffective in H_2O,[31] thus often requiring pretreatment to remove water from the air and inducing additional cost to the operation of DAC.

Degradation assessment under accelerated ageing

We evaluated the sorbents stability through accelerated ageing by exposing the materials to ambient air at 85 °C for 7 days. The accelerated ageing conditions are harsh and correspond to over 2000 regeneration cycles, based on 5 minutes desorption durations reported in literature for TGA assessments.[50]

Fig. 5 shows the changes in CO_2 capture capacity of the sorbents before and after accelerated ageing, with 0.5DEA&0.5TEA@SAN and 0.5DEA&0.5MDEA@SAN as the representatives of Class IV sorbents. The capacity of 0.5DEA&0.5TEA@SAN remained the same as the pristine

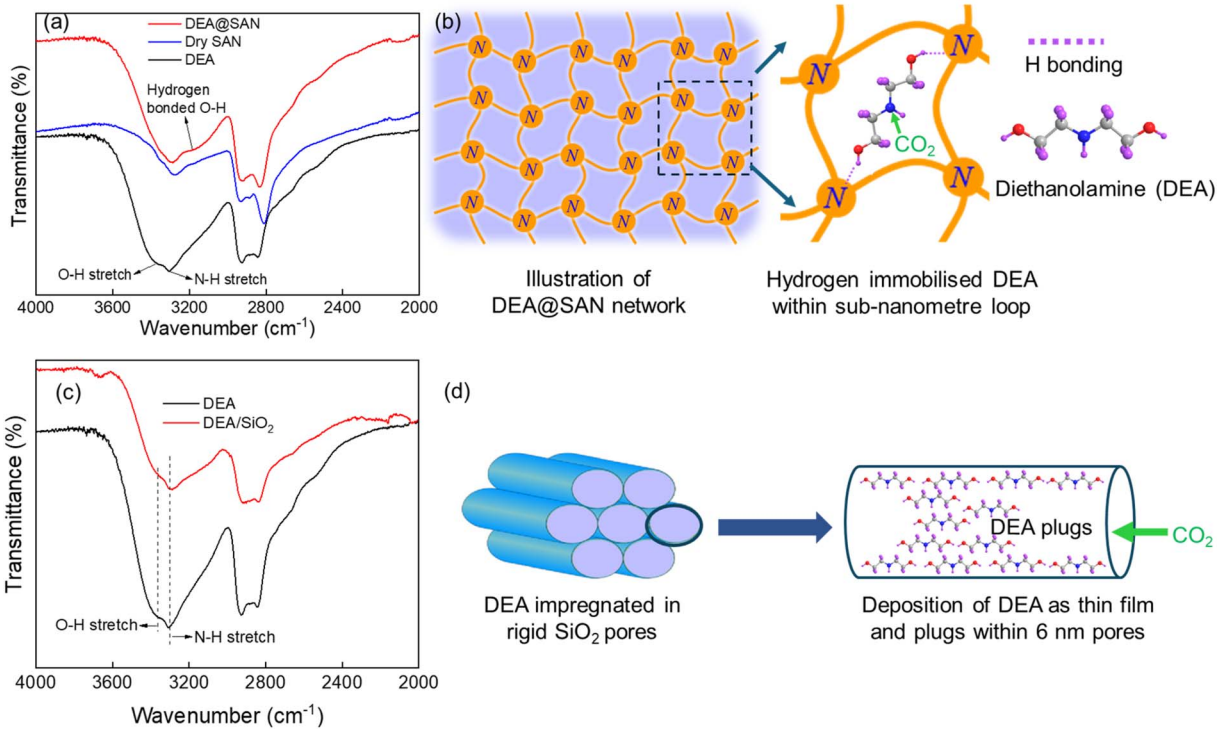

Fig. 4 Interactions of DEA with structurally different SAN and SiO_2. (a) IR spectra showing formation of hydrogen bonding between DEA and SAN; (b) illustrative conceptual representation of SAN network with sub-nanometre loops that exert a strong confinement effect on DEA; (c) IR spectra showing no obvious changes to DEA when impregnated into SiO_2; (d) deposition of DEA in SiO_2 pores, forming plugs and thus low efficiency.

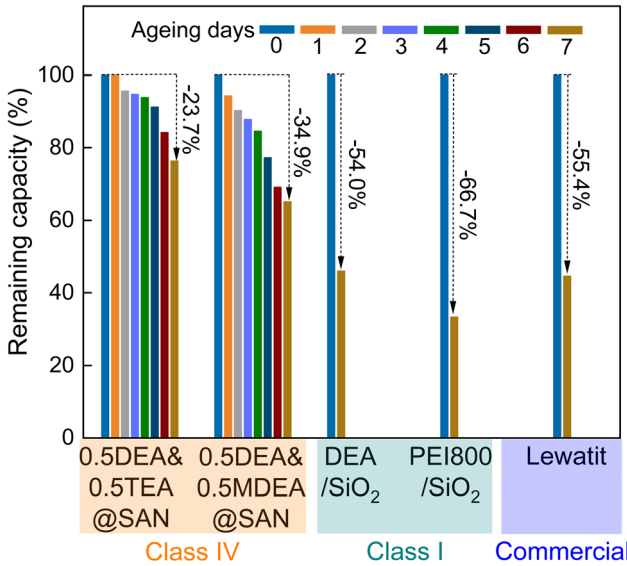

Fig. 5 Reduction in capture capacity of Class IV sorbents compared to conventional SiO_2 impregnated counterparts and Lewatit resin after accelerated ageing. The CO_2 capture performance was evaluated using atmospheric air under ambient temperature. The accelerated ageing was conducted at 85 °C in air for 7 days.

counterpart after the first day ageing and decreased gradually thereafter, resulting in 23.7% reduction at the end of the accelerated ageing. A similar trend was also observed for 0.5DEA&0.5MDEA@SAN which incurred 34.9% reduction compared to its original capacity. In a different scenario, the two Class I sorbents (DEA/SiO_2 and PEI800/SiO_2) as well as the commercially available Lewatit resin which all exhibited significant reduction in capacity by the seventh day of ageing, double than that of the 0.5DEA&0.5TEA@SAN sorbent. Although PEI800/SiO_2 demonstrated a desirable CO_2 uptake of 2.34 mmol g^{-1}, it reduced by 66.7% to only 0.75 mmol g^{-1} after ageing. Under the same ageing conditions, 0.5DEA&0.5TEA@-SAN still possessed capture capacity of 1.93 mmol g^{-1}, comparable to the as synthesized COF-999 (2.05 mmol g^{-1}),[46] and higher than many sorbents reported in the literature. The CO_2 uptakes as a function of adsorption time for each sorbent before and after the ageing are shown in Fig. S14–S18.

Amine-based sorbents are known to be susceptible to degradation due to oxidation particularly at high temperatures.[51] Class IV sorbents show increased resistance to oxidation compared to other counterparts. This is also reflected in the changes in FTIR spectrum before and after the ageing as shown in Fig. S19–S21. After ageing all sorbents displayed a new peak around 1650 cm^{-1} owing to the IR absorption from C=O stretching,[14,51] suggesting the generation of new functional groups which are attributed to oxidation. The intensity of the new peak is less for 0.5DEA&0.5TEA@SAN but more pronounced for PEI800/SiO_2, in line with the extent of their reduction in capture capacity as discussed above.

The high stability of 0.5DEA&0.5TEA@SAN can be rationalised by the unique structure of the SAN. Epoxides have been reported to effectively enhance the stability of PEI through converting primary amines to secondary amines.[14,52] In this work, TGIC with three epoxy groups not only enabled the crosslinking reaction with PEI but also reduced the amount of primary amine groups, decreasing the susceptibility of the resulted SAN to oxidation. In addition, with nano-confinement through strong hydrogen bonding, the amines incorporated into the network are immobilised and thus further stabilised, as seen in many examples such as catalysis and biological systems.[53] As a result, Class IV sorbents demonstrates outstanding stability compared to their Class I counterparts. It should be noted that TSP can also contribute to the improved stability owing to its iron chelating effect.[14] It is expected the longevity of the Class IV sorbents can be significantly enhanced if vacuum is utilised to assist the desorption, in a way that the sorbent is exposed to low-level oxygen.

DAC under real-world conditions

One of the advantages of DAC is that it is not geographically restricted, allowing facilities to be located where renewable energy can be utilised more efficiently. We demonstrated the feasibility of solar-assisted DAC by assessing the performance of 0.5DEA&0.5TEA@SAN exposed to outdoor ambient air as shown in Fig. 6a. The sorbent captured ambient CO_2 through the air accelerated by a fan powered by solar. The weather was mostly sunny with temperature in the range of 17 to 21 °C and relative humidity around 70%. Such operational efficiency would not be possible for liquid sorbents.

The quantities of CO_2 desorbed from samples after various capture durations are presented in Fig. 6b. A small amount of CO_2 was released from the freshly regenerated sample, which could be attributed to CO_2 captured during sample loading to TGA. With increasing capture time, more CO_2 was released from the sample, suggesting that more CO_2 was captured with long exposure time. It is also found that CO_2 start to desorb at temperatures as low as 40 °C, and the desorption can be completed with temperature below 90 °C, in line with the CO_2 desorption profiles measured by TGA-MS illustrated in Fig. S22. This is a significant reduction in regeneration temperature compared to 900 °C required for metal hydroxide-based sorbent, which is crucial for the deployment of DAC to substantially reduce energy consumption and cost.

Fig. 6c illustrates the accumulated amount of CO_2 released at different capture times. 0.37 mmol g^{-1} CO_2 was desorbed within capture time as short as 1 h, and 0.98 mmol g^{-1} CO_2 was released by 5 h adsorption, equivalent to 4.33 wt% CO_2 captured. This closely matches with the CO_2 uptake as a function of time for 0.5DEA&0.5TEA@SAN assessed using the in-house built DAC instrument, as shown in Fig. S23, suggesting the CO_2 captured can be also readily released by thermal desorption. This reveals the capture of 0.65 g of CO_2 in 5 h from air by the 15 g of 0.5DEA&0.5TEA@SAN used. Assuming an adsorption of 5 h and a desorption of 1 h per DAC cycle, corresponding to 4 cycles a day, 1 tonne of CO_2 can be captured daily using 5.77 tonnes of sorbent. Given the density of sorbent as 0.48 g mL^{-1}, this corresponds to a volume of 12 m^3, which is only 1/3 of a standard shipping container. This is significant for

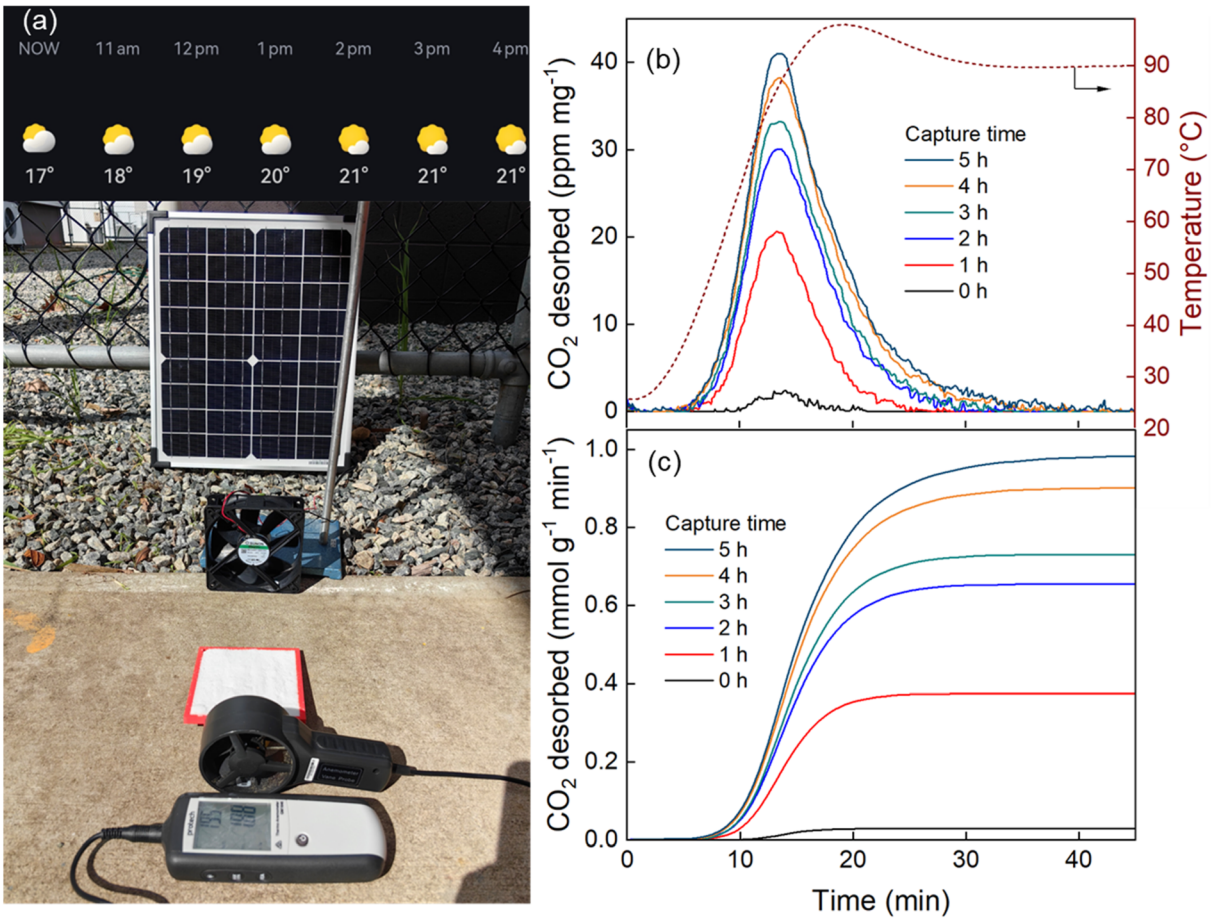

Fig. 6 Solar assisted DAC under real-world conditions by exposing the sorbent to outdoor ambient air for 5 hours. (a) Setup of the DAC system consists of a solar panel to power a computer fan blowing air over 15 g of sorbents at a wind speed about 2 m s^{-1}; (b) concentrations of CO_2 desorbed from the sorbents at different capture time. The desorption was performed using TGA with temperature up to 90 °C, and the released CO_2 concentrations were recorded using a Vaisala CO_2 sensor; (c) accumulated CO_2 concentrations at different capture time demonstrate nearly 1 mmol g^{-1} CO_2 captured within 5 hours, indication high efficiency of the sorbent in DAC.

the widespread deployment of DAC with annual capture capacity expected to be in the megatons range. We demonstrated the feasibility of solar-assisted DAC using Class IV sorbent, conforming with the advantages of solid sorbent-based DAC with no geographical restriction that can utilise renewable energy more effectively.

Conclusions

We have presented a novel, efficient method for synthesising a new class of sorbent material (SAN) for CO_2 removal *via* direct air capture (DAC). The sorbents were produced through a one-pot, autocatalytic process using widely available reactants, conducted under ambient conditions and completed in just 10 minutes. The process aligns with green chemistry principles, as it generates no waste, requires no post-treatment, and integrates all reactants into the final product, enabling large-scale production.

The sorbent demonstrates exceptional performance in capturing ultralow concentrations of CO_2 from the atmosphere and outperformed most previously reported sorbents as well as a commercially available counterpart. Additionally, the sorbent has high tolerance to water allowing it to operate effectively in outdoor ambient air. Its unique structure enables a strong confinement effect and interaction between the network and the confined amine, resulting in sorbents with both remarkable CO_2 capture capacity and unprecedented resistance to oxidative degradation. The SAN sorbent exhibited a CO_2 uptake of 3.11 mmol g^{-1} which is one of the highest recorded in such settings. It also retained over 75% of its capacity after one week of accelerated ageing at 85 °C in air, far exceeding the conventional Class I sorbents and a commercially available alternative, which lose over 50% of their capacity under similar conditions.

Exposing 15 g of sorbents to outdoor air under real-world DAC conditions represents a significant advancement, marking one of the first demonstrations of a simple, renewable-energy-powered capture process. With its ease of production, high CO_2 capture capacity and stability, low CO_2 desorption temperature, and high tolerance for water, this study addresses several often-overlooked challenges in scaling DAC sorbents.

This study has notable implications for (i) the academic community: it presents a new approach to designing solid DAC

sorbents without relying on porous materials, with the versatility of crosslinkers and amines offers opportunities to develop a variety of materials with applications extending beyond DAC; (ii) industry: our sorbent is among the few that can be manufactured at scale in an eco-friendly and cost-effective manner which is a critical point highlighted in several major reports.

Author contributions

Z. Wan and C. D. Wood conceived the research idea. Z. Wan conducted the sorbents synthesis, carried out the performance assessment of the sorbents in DAC, collected and analysed TGA-CO_2 sensor data, and analysed the FTIR data with great help from B. Pejcic. W. Tian performed the thermoporometry and assisted data analysis. D. Acharya carried out PALS measurements and assisted data analysis. S. Surin conducted the TGA-MS and assisted data analysis. W. Wu helped with the graphical abstract. Z. Wan prepared the initial draft with valuable suggestions and revisions from C. White, J. Czapla, B. Pejcic and C. D. Wood, and finalised the manuscript with C. D. Wood for submission.

Conflicts of interest

The authors declare no competing interests.

Data availability

Data for this article, including testing results, FTIR and TGA-MS are available at Science Data Bank at http://doi.org/10.57760/sciencedb.29846.

Supplementary information (SI) is available. See DOI: https://doi.org/10.1039/d5ta10113a.

Acknowledgements

The authors gratefully acknowledge the financial support from the Commonwealth Scientific and Industrial Research Organisation (CSIRO). The authors also want to thank Dr Gongkui Xiao and Shailza Sharma for performing the nitrogen physisorption measurements.

Notes and references

1 X. Xu, M. B. Myers, F. G. Versteeg, B. Pejcic, C. Heath and C. D. Wood, *Chem. Commun.*, 2020, **56**, 7151–7154.
2 X. Shi, H. Xiao, H. Azarabadi, J. Song, X. Wu, X. Chen and K. S. Lackner, *Angew. Chem., Int. Ed.*, 2020, **59**, 6984–7006.
3 A. H. Berger, M. T. McDonald and A. Bhown, Overcoming Barriers to Deploying Direct Air Capture: Conclusions from a Workshop with Leaders in the Field, in *Proceedings of the 16th Greenhouse Gas Control Technologies Conference (GHGT-16)*, 2022, pp. 23–24.
4 K. Sievert, T. S. Schmidt and B. Steffen, *Joule*, 2024, **8**, 979–999.
5 H. Bouaboula, J. Chaouki, Y. Belmabkhout and A. Zaabout, *Chem. Eng. J.*, 2024, **484**, 149411.
6 G. T. Rochelle, in *Absorption-Based Post-combustion Capture of Carbon Dioxide*, ed. P. H. M. Feron, Woodhead Publishing, 2016, pp. 35–67, DOI: 10.1016/B978-0-08-100514-9.00003-2.
7 X. Xu, M. B. Myers, F. G. Versteeg, E. Adam, C. White, E. Crooke and C. D. Wood, *J. Mater. Chem. A*, 2021, **9**, 1692–1704.
8 B. Dutcher, M. Fan and A. G. Russell, *ACS Appl. Mater. Interfaces*, 2015, **7**, 2137–2148.
9 H. A. Patel, J. Byun and C. T. Yavuz, *ChemSusChem*, 2017, **10**, 1303–1317.
10 R. L. Siegelman, E. J. Kim and J. R. Long, *Nat. Mater.*, 2021, **20**, 1060–1072.
11 X. Zhu, W. Xie, J. Wu, Y. Miao, C. Xiang, C. Chen, B. Ge, Z. Gan, F. Yang, M. Zhang, D. O'Hare, J. Li, T. Ge and R. Wang, *Chem. Soc. Rev.*, 2022, **51**, 6574–6651.
12 D. Panda, V. Kulkarni and S. K. Singh, *React. Chem. Eng.*, 2023, **8**, 10–40.
13 S. H. Pang, R. P. Lively and C. W. Jones, *ChemSusChem*, 2018, **11**, 2628–2637.
14 K. Min, W. Choi, C. Kim and M. Choi, *Nat. Commun.*, 2018, **9**, 726.
15 P. D. Jadhav, R. V. Chatti, R. B. Biniwale, N. K. Labhsetwar, S. Devotta and S. S. Rayalu, *Energy Fuels*, 2007, **21**, 3555–3559.
16 H. Thakkar, A. Issa, A. A. Rownaghi and F. Rezaei, *Chem. Eng. Technol.*, 2017, **40**, 1999–2007.
17 Z. Chen, S. Deng, H. Wei, B. Wang, J. Huang and G. Yu, *ACS Appl. Mater. Interfaces*, 2013, **5**, 6937–6945.
18 G. Rim, F. Kong, M. Song, C. Rosu, P. Priyadarshini, R. P. Lively and C. W. Jones, *JACS Au*, 2022, **2**, 380–393.
19 G. Rim, P. Priyadarshini, M. Song, Y. Wang, A. Bai, M. J. Realff, R. P. Lively and C. W. Jones, *J. Am. Chem. Soc.*, 2023, **145**, 7190–7204.
20 J. C. Hicks, J. H. Drese, D. J. Fauth, M. L. Gray, G. Qi and C. W. Jones, *J. Am. Chem. Soc.*, 2008, **130**, 2902–2903.
21 J.-T. Anyanwu, Y. Wang and R. T. Yang, *Chem. Eng. Sci.*, 2022, **254**, 117626.
22 S. Choi, J. H. Drese, P. M. Eisenberger and C. W. Jones, *Environ. Sci. Technol.*, 2011, **45**, 2420–2427.
23 X. Xu, C. Song, J. M. Andresen, B. G. Miller and A. W. Scaroni, *Energy Fuels*, 2002, **16**, 1463–1469.
24 Y. Miao, Z. He, X. Zhu, D. Izikowitz and J. Li, *Chem. Eng. J.*, 2021, **426**, 131875.
25 J. Wang, X. Feng, S. Wen, D. Zhan, X. Zhu, P. Ning, Y. Zhang and X. Mei, *Renewable Sustainable Energy Rev.*, 2024, **203**, 114724.
26 E. S. Sanz-Pérez, A. Fernández, A. Arencibia, G. Calleja and R. Sanz, *Chem. Eng. J.*, 2019, **373**, 1286–1294.
27 B. Wadi, A. Golmakani, V. Manovic and S. A. Nabavi, *Ind. Eng. Chem. Res.*, 2021, **60**, 13309–13317.
28 L. B. Hamdy, R. J. Wakeham, M. Taddei, A. R. Barron and E. Andreoli, *Chem. Mater.*, 2019, **31**, 4673–4684.
29 C.-J. Yoo, P. Narayanan and C. W. Jones, *J. Mater. Chem. A*, 2019, **7**, 19513–19521.
30 P. Narayanan, R. P. Lively and C. W. Jones, *Energy Fuels*, 2023, **37**, 5257–5269.

31 Z. Wan, R. Hunt, C. White, J. Gillbanks, J. Czapla, G. Xiao, S. Surin and C. Wood, *ChemSusChem*, 2024, e202400212.
32 P. T. Anastas and J. C. Warner, *Green Chemistry: Theory and Practice*, 1998, vol. 29, pp. 14821–14842.
33 C. Zhao, Y. Guo, W. Li, C. Bu, X. Wang and P. Lu, *Chem. Eng. J.*, 2017, **312**, 50–58.
34 S. Mukherjee and A. N. Samanta, *Adv. Powder Technol.*, 2019, **30**, 3231–3240.
35 A. R. Katritzky, C. A. Ramsden, J. A. Joule and V. V. Zhdankin, *Handbook of Heterocyclic Chemistry*, 2010, pp. 210–237, DOI: 10.1016/B978-0-08-095843-9.00006-9.
36 X. Xu, B. Pejcic, C. Heath, M. B. Myers, C. Doherty, Y. Gozukara and C. D. Wood, *ACS Appl. Mater. Interfaces*, 2019, **11**, 26770–26780.
37 Y. Du, X. Xue, Q. Jiang, W. Huang, H. Yang, L. Jiang, B. Jiang and S. Komarneni, *Polym. Chem.*, 2023, **14**, 3679–3685.
38 J. L. Han, K. H. Hsieh and W. Y. Chiu, *J. Appl. Polym. Sci.*, 1993, **50**, 1099–1106.
39 C. M. Sahagun, K. M. Knauer and S. E. Morgan, *J. Appl. Polym. Sci.*, 2012, **126**, 1394–1405.
40 A. Shundo, S. Yamamoto and K. Tanaka, *JACS Au*, 2022, **2**, 1522–1542.
41 M. R. Landry, *Thermochim. Acta*, 2005, **433**, 27–50.
42 D. Majda, W. Makowski and M. Mańko, *J. Therm. Anal. Calorim.*, 2012, **109**, 663–669.
43 M. Tanaka, T. Motomura, N. Ishii, K. Shimura, M. Onishi, A. Mochizuki and T. Hatakeyama, *Polym. Int.*, 2000, **49**, 1709–1713.
44 V. M. Gun'ko, I. N. Savina and S. V. Mikhalovsky, *Gels*, 2017, **3**, 37.
45 H. J. Moon, J. Y. Carrillo, M. Song, G. Rim, W. T. Heller, J. Leisen, L. Proano, G. N. Short, S. Banerjee, B. G. Sumpter and C. W. Jones, *ChemSusChem*, 2024, e202400967.
46 Z. Zhou, T. Ma, H. Zhang, S. Chheda, H. Li, K. Wang, S. Ehrling, R. Giovine, C. Li, A. H. Alawadhi, M. M. Abduljawad, M. O. Alawad, L. Gagliardi, J. Sauer and O. M. Yaghi, *Nature*, 2024, **635**(8037), 96–101.
47 T. S. Nguyen, N. A. Dogan, H. Lim and C. T. Yavuz, *Acc. Chem. Res.*, 2023, **56**, 2642–2652.
48 H. J. Moon, J. M. Y. Carrillo and C. W. Jones, *Acc. Chem. Res.*, 2023, **56**, 2620–2630.
49 A. Holewinski, M. A. Sakwa-Novak and C. W. Jones, *J. Am. Chem. Soc.*, 2015, **137**, 11749–11759.
50 A. Goeppert, H. Zhang, R. Sen, H. Dang and G. K. S. Prakash, *ChemSusChem*, 2019, **12**, 1712–1723.
51 J. S. A. Carneiro, G. Innocenti, H. J. Moon, Y. Guta, L. Proaño, C. Sievers, M. A. Sakwa-Novak, E. W. Ping and C. W. Jones, *Angew. Chem., Int. Ed.*, 2023, **62**, e202302887.
52 W. Choi, K. Min, C. Kim, Y. S. Ko, J. Jeon, H. Seo, Y. K. Park and M. Choi, *Nat. Commun.*, 2016, **7**, 12640.
53 A. B. Grommet, M. Feller and R. Klajn, *Nat. Nanotechnol.*, 2020, **15**, 256–271.